Propagation Modes and Dispersion Characteristics of Coplanar Waveguides

MAJID RIAZIAT, MEMBER, IEEE, REZA MAJIDI-AHY, MEMBER, IEEE, AND I-JAUNG FENG

Abstract—**The coplanar waveguide structure is subdivided into five classes based on substrate thickness, backside metallization, and ground plane width. Radiation and guided modes are studied in each class, and their effects on loss and dispersion are described.**

I. Introduction

SINCE the adoption of coplanar waveguide (CPW) in certain MMIC applications [1]–[3], the need for an in-depth analysis of this structure has increased. In particular, dispersion and discontinuity models are needed for CPW in order to further expand its use in monolithic circuits. Numerical techniques have been used to model propagation [4], loss [5], and moding behavior in specific CPW structures [6]. A limited number of analytical results also exists on the subject, mainly dealing with characteristic impedance and propagation constant calculations of ideal modes [7], [8]. The present work is an attempt to study the basics of wave propagation in coplanar waveguides for the purpose of facilitating more complete modeling efforts and providing guidelines for MMIC design using this medium.

A coplanar waveguide in its ideal form consists of a conducting strip with two semi-infinite side conductors on the surface of an infinitely thick dielectric substrate (Fig. 1). Practical realizations of CPW deviate from this definition in a number of ways. First, in most cases, the substrate cannot be considered infinitely thick. Second, the side conductors have finite widths. Third, the finite substrate may have a conducting back plate. Variations in these three parameters lead to five practical cases with different propagating modes and dispersion characteristics that will be discussed separately.

Transverse confinement of the fields as well as the presence of a top cover, which occurs in packaged circuits [9], [10], requires additional analysis. These packaging issues are not addressed here.

II. Infinite Substrate

Guided modes of the ideal CPW structure have been studied by a number of authors [11], [12]. The ideal CPW structure is conveniently considered as a pair of coupled slotlines with odd and even normal modes. The odd and even modes are what we refer to as the CPW mode and the slot line mode, respectively. This is to avoid confusion, especially in the presence of additional modes.

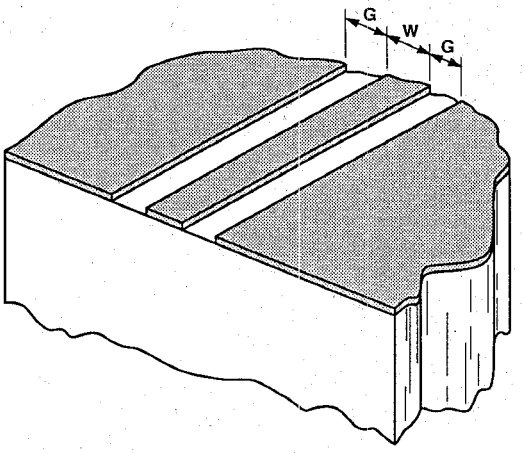

Fig. 1. The ideal coplanar waveguide structure.

The CPW guided mode propagates at the interface between two dielectric media with a phase velocity v_g that exceeds that of a TEM wave in the higher dielectric constant material (v_d). This condition gives rise to radiation from the guided CPW wave into the substrate. For constructive interference, the radiated wave and the guided CPW wave should have the same propagation constant along the direction of the CPW transmission line. This requirement restricts the propagation direction of the radiated wave to a semicone of angle θ, given by

$$\cos\theta = k_g/k_d = (\epsilon_{\text{eff}}/\epsilon_r)^{1/2} \tag{1}$$

where k_g and k_d are the propagation constants of the guided and radiated waves respectively. Energy transfer from the CPW mode into the substrate causes attenuation of the guided wave. The attenuation constant α as calculated by Rutledge *et al.* [13] is given by

$$\alpha = f(\epsilon_r)\left(\frac{1}{\lambda_d}\right)^3 \frac{(W+2G)^2}{K(k)K'(k)} \tag{2}$$

in units of inverse length; $k = W/(W+2G)$, K, and K' are complete elliptic integrals of the first and second kinds,

Manuscript received April 10, 1989; revised October 17, 1989.
The authors are with the Varian Research Center, 611 Hansen Way, Palo Alto, CA 94303.
IEEE Log Number 8933247.

0018-9480/90/0300–0245$01.00 ©1990 IEEE

and

$$f(\epsilon_r) = \left(\frac{\pi}{2}\right)^5 \frac{1}{\sqrt{2}} \frac{(1-1/\epsilon_r)^2}{\sqrt{1+1/\epsilon_r}}. \tag{3}$$

For GaAs substrates, this expression reduces to

$$\alpha = \frac{47.4}{K(k)K'(k)} \left(\frac{W+2G}{\lambda_d}\right)^2 \tag{4}$$

in units of dB (per λ_d).

A 50 Ω CPW on GaAs has a k value of 0.5, for which $K(k)K'(k) = 3.44$ and varies slowly with k. Substituting this in (4) gives

$$\alpha = 13.8 \left(\frac{W+2G}{\lambda_d}\right)^2. \tag{5}$$

For $(W+2G) \leqslant \lambda_d/20$, attenuation due to radiation is less than 0.034 dB per dielectric wavelength, which is easily acceptable for integrated circuit applications.

III. Finite Substrate Without Back-Side Metallization

When substrate thickness is comparable to dielectric wavelength, reflections from the back-plane air–dielectric interface should also be taken into account. The problem is that of a conductor-backed dielectric slab (Fig. 2(a)). Surface wave modes of this structure are odd TE modes and even TM modes of a dielectric slab with twice the thickness and no metallization [14], where odd and even refer to the symmetry of the transverse field component. These modes (sometimes referred to as grounded slab modes) are similar to the ones encountered in the case of microstrip lines. The interaction of the CPW mode with the surface waves, however, is different from that of microstrip due to the difference in their field distributions. Most CPW structures have less field overlap with surface wave modes than microstrip, and interact weakly with them (see the section on dispersion effects). Despite this weak interaction, in frequency ranges where the propagation constants of the surface waves approach or exceed that of the CPW mode, considerable dispersion and radiative losses can occur.

TE and TM modes of the conductor-backed dielectric slab are shown in Fig. 3. For comparison, the normalized propagation constant range for the CPW mode, corresponding to $\epsilon_{\text{eff}}/\epsilon_r$ ranging from 0.48 to 0.64, is also shown. This range corresponds to the values most commonly encountered in monolithic circuits on GaAs. At low frequencies, where the phase velocity of the surface wave mode is much higher than the CPW mode, only weak dispersion effects are observed. As the frequency increases the phase velocity of the surface wave mode approaches and eventually becomes less than that of the CPW mode. Close to the point of intersection the two modes are synchronous (i.e., phase matched) and interact strongly, resulting in a highly dispersive behavior near this frequency. Above this point the surface wave mode mainly

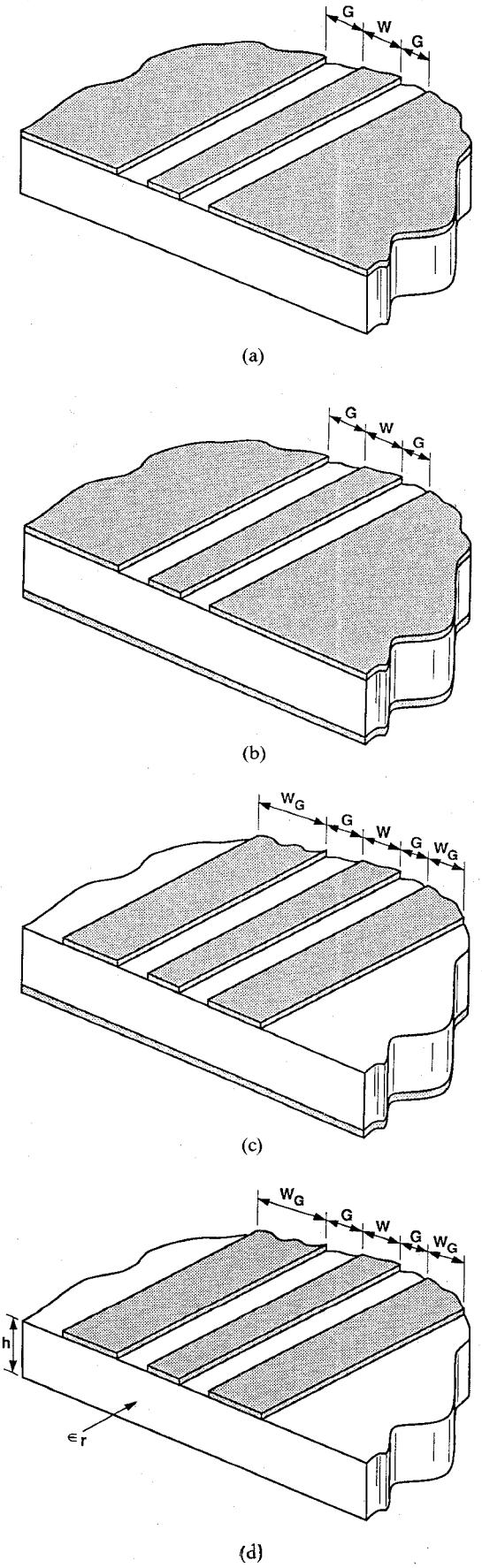

Fig. 2. Practical coplanar waveguide structures: (a) finite substrate, (b) finite substrate with back-side metallization, (c) finite ground planes, (d) finite ground planes without back-side metallization.

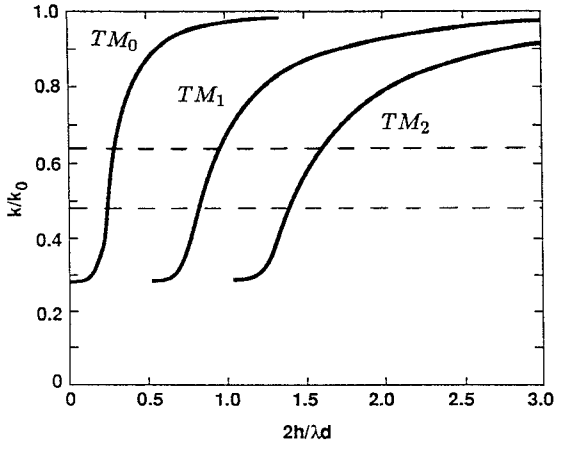

(a)

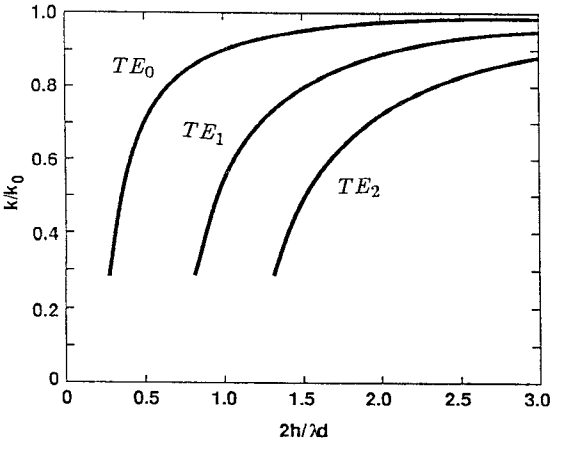

(b)

Fig. 3. Surface wave modes in a conductor-backed dielectric slab of thickness h: (a) transverse magnetic, (b) transverse electric.

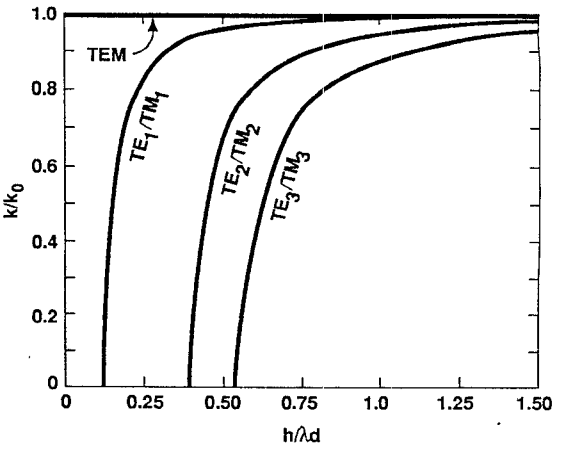

Fig. 4. Parallel-plate waveguide modes for a dielectric slab metallized on both sides.

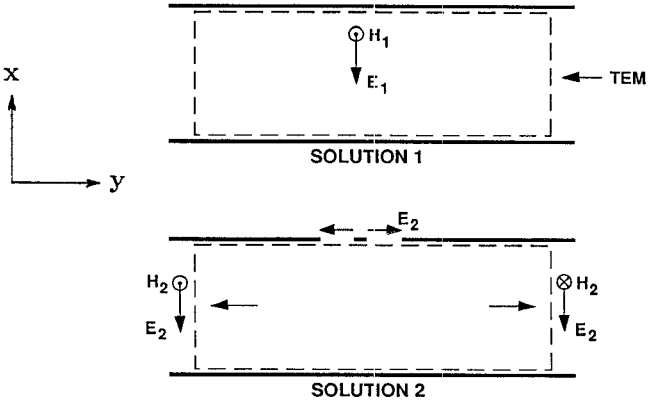

Fig. 5. Electromagnetic field solutions chosen for calculation of CPW radiation into the parallel-plate waveguide mode.

contributes to loss in the CPW mode, which keeps increasing with frequency. For wide-band integrated circuit applications it may be advantageous to select the substrate thickness such that the operating frequency range is below this intersection point. For the lowest order TM mode this requirement is satisfied if $h < 0.15\lambda_d$ (Fig. 3(a)).

The next mode that can be excited as the frequency is increased is the TE_0 mode whose cutoff frequency is at $2h \approx 0.25\lambda_d$. This mode will by synchronous with the CPW mode near $2h = 0.35\lambda_d$ (Fig. 3(b)). A conservative guideline to avoid all potential problem points is to operate below the cutoff frequency of the TE_0 mode, i.e., $h < 0.12\lambda_d$. This guideline is also valid for microstrip since the same substrate modes are involved.

IV. Finite Substrate with Back-Side Metallization

In many applications of coplanar waveguide MIC's, the substrate has a conducting surface on the back side, due to either intentional metallization or mounting in a metal housing. Back-side metallization of the substrate together with wide top-side ground planes (Fig. 2(b)) gives rise to parallel-plate waveguide modes. What is significantly different in this case compared to the unmetallized substrate is the presence of a zero cutoff TEM mode (Fig. 4). The phase velocity of this mode is smaller than the CPW mode, and therefore constitutes a source of power loss for CPW in the absence of lateral confinement. It should be kept in mind that lateral confinement of this structure gives rise to dispersion effects associated with rectangular waveguide modes. In this section we will use the reciprocity theorem to derive an expression for the functional dependence of power loss due to radiation in the TEM parallel-plate mode.

The reciprocity theorem in a simple form is given by

$$\oint \left(\vec{E}_1 \times \vec{H}_2 - \vec{E}_2 \times \vec{H}_1 \right) \cdot d\vec{s} = 0 \qquad (6)$$

over any closed surface. Subscripts 1 and 2 refer to two electromagnetic field solutions over the region of interest. Fig. 5 shows the two solutions picked for this calculation. Solution 1 is a TEM wave propagating from right to left in the absence of the transmission line. Solution 2 is the TEM mode propagating away from the CPW at an angle θ with

the z axis given by (1). The integration surface is also shown in the figure. It can be seen that the only contributions to the surface integral come from the cross section of the CPW and the two end surfaces, which are taken to be far from the transmission line. Therefore,

$$\int_{\substack{\text{TRL cross}\\ \text{section}}} \left(\vec{E}_1 \times \vec{H}_2 - \vec{E}_2 \times \vec{H}_1\right) \cdot d\vec{s} = -\int_{\substack{\text{left and}\\ \text{right surfaces}}} \left(\vec{E}_1 \times \vec{H}_2 - \vec{E}_2 \times \vec{H}_1\right) \cdot d\vec{s}. \quad (7)$$

The contributions of $\vec{E}_2 \times \vec{H}_1$ on the left and right surfaces cancel each other. The remaining integral is related to the radiated power, which is the quantity of interest. Also, the left-hand side of the equation simplifies further, noting that $\vec{E}_1$ has no tangential component over the cross section of the transmission line. The result is

$$2\int_{\text{right hand surface}} \left(\vec{E}_1 \times \vec{H}_2\right) \cdot d\vec{s} = \int_{-(W+2G)/2}^{(W+2G)/2} (E_{y2})(H_{z1})\, dy. \quad (8)$$

If $W+2G$ is small compared to the wavelength, the integrations result in the following expression for the power attenuation constant α, defined as the ratio of radiated power to twice the guided power per unit length:

$$\alpha = \frac{\pi^2}{2h} \frac{Z_0}{\eta_d} \frac{(W+2G)^2}{(\lambda_d)^2} \sqrt{1-\epsilon_{\text{eff}}/\epsilon_r}. \quad (9)$$

Here, Z_0 is the CPW impedance, and $\eta_d = 377/\sqrt{\epsilon_r}$ is the wave impedance of the dielectric material.

Radiation from the CPW mode is much less than from the slotline mode, mainly because in the CPW mode the electric fields (or the equivalent magnetic currents) point in opposite directions, causing partial cancellation and a second-order dependence of the radiated power on $(W+2G)$. For a 50 Ω CPW line on GaAs with $(W+2G) = h/4 \leqslant \lambda_d/20$, attenuation is less than 0.17 dB per guide wavelength. This value also gives a qualitative estimate of the maximum level of cross talk and interference, through coupling with the parallel-plate TEM mode, that can be expected in a CPW integrated circuit with back-side metallization.

The next higher order modes of the parallel-plate waveguide are TE_1 and TM_1 modes, which will be synchronous with CPW near $h = 0.125\lambda_d$. Therefore the previously established criterion of $h < 0.12\lambda_d$ also avoids the higher order parallel-plate waveguide modes.

V. Finite Substrate and Finite Ground Planes Without Back-Side Metallization

A large area of substrate material is exposed in this case without any metallization on either side (Fig. 2(d)). This portion of the substrate supports full slab modes, including zero cutoff TE_0 and TM_0 modes. The first substrate mode to start interacting with the CPW mode is TE_0, whose characteristics are given in Fig. 6. Dispersion caused by the presence of TE_0 and TM_0 modes is unavoidable at any frequency, but the region where TE_0 has a phase velocity close to that of the CPW mode can be avoided if the criterion $h < 0.1\lambda_d$ is met ($k/k_0 < 0.48$ in Fig. 6). This is a slightly more stringent requirement than encountered in other cases and justifies avoiding large areas of exposed substrate in close proximity to a CPW line.

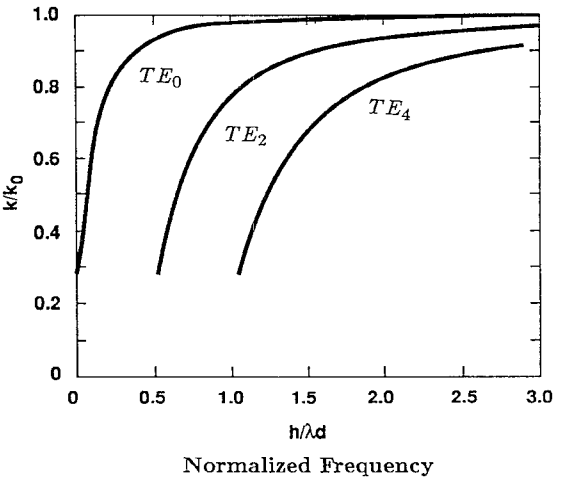

Fig. 6. Even TE modes in a dielectric slab with no metallization on either side.

VI. Finite Substrate and Finite Ground Planes with Back-Side Metallization

Finite ground planes on finite substrate with back-side metallization behave as microstrip lines coupled together and to the center conductor (Fig. 2(c)). The propagation modes on this structure are not as simple as the odd and even modes of the ideal CPW. In fact, none of the normal modes of this structure allow both ground planes to remain at zero potential [15]. This can cause significant problems in a circuit designed with CPW.

Three coupled microstrips have three normal modes of propagation. Each mode is represented by a three-dimensional vector, with elements representing relative potentials on the three lines [16]. The relative potentials remain the same as the mode propagates along the line. This is not the case if the transmission line is excited with three arbitrary voltages. For example, the excitation

$$V_0 = \begin{pmatrix} 0 \\ 1 \\ 0 \end{pmatrix}$$

represents a signal on the center conductor with the side conductors at zero potential. This is not a normal mode of the structure, which means the relationships between the three potentials on the line will change as the excitation propagates. The three normal modes are given by [15]

$$V_1 = \begin{pmatrix} -1 \\ 0 \\ +1 \end{pmatrix} \quad V_2 = \begin{pmatrix} a \\ 1 \\ a \end{pmatrix} \quad V_3 = \begin{pmatrix} -b \\ 1 \\ -b \end{pmatrix}. \quad (10)$$

V_1 is the slotline mode, which corresponds to the well-

known even mode of CPW on a semi-infinite substrate. This is a non-TEM mode orthogonal to V_0. The slotline mode is normally suppressed in most applications [1]. The other two modes, V_2 and V_3, are the microstrip mode and the coplanar mode, respectively. These modes involve parameters a and b, which are functions of the physical dimensions of the line. In general $a \neq b$ and the phase velocities associated with these modes are different. The

$$\begin{pmatrix} 0 \\ 1 \\ 0 \end{pmatrix}$$

excitation is a combination of V_2 and V_3:

$$\begin{pmatrix} 0 \\ 1 \\ 0 \end{pmatrix} = \frac{1}{(a+b)} \left[b \begin{pmatrix} a \\ 1 \\ a \end{pmatrix} + a \begin{pmatrix} -b \\ 1 \\ -b \end{pmatrix} \right]. \tag{11}$$

Since the phase velocities v_2 and v_3 associated with modes V_2 and V_3 are different, the phase angle between the constituent modes of V_0 will drift along the transmission line, and finite potentials will appear on the ground planes.

It is desirable in most applications to design the CPW in a way that would allow only the single propagating signal V_0. Although V_0 is not a normal mode, if the ground plane width W_g and the substrate thickness h are chosen to be larger than the line width $W+2G$, the coplanar mode V_3 will approach V_0; i.e., the value of b becomes much smaller than 1.

In order to demonstrate this numerically, three line geometries were chosen for which the normal modes were calculated [15]. The parameters h and W_g were varied among the three lines, while ϵ_r, W, and G remained fixed at 12, 50 μm, and 25 μm respectively.

For the first line, substrate thickness was $h = 100$ μm, with a ground plane width of $W_g = 200$ μm. The value of b for the coplanar mode was calculated to be 0.156, corresponding to a signal level of the ground plane, 16 dB below the center conductor. For the second line the substrate thickness was increased to 400 μm keeping all the other parameters the same. The value of b was reduced to 0.122, or 18 dB below the center conductor. For the third line all parameters were the same as the second line, except the ground plane width, which was increased from 200 to 400 μm. The value of b was further reduced to 0.06, or 24 dB below the center conductor.

The above analysis shows that in the coplanar mode, the potential on the ground planes can be kept close to zero if the criteria of wide ground planes and thick substrate compared to $W+2G$ are met. It should also be pointed out that once the signal V_0 has been excited on the transmission line, the maximum potential on the ground plane appears at a distance equal to half the beat wavelength between microstrip and coplanar modes. For the three lines considered, this distance varies from 8.7 to 10.5 mm at the frequency of 30 GHz. In MMIC applications, where uninterrupted propagation distances are generally much less than this, problems encountered are due not to the fact that V_0 excitation is not a pure mode but rather to unintentional excitation of the microstrip mode at the launch point. This is likely to occur at transitions between microstrip and CPW. For a more detailed discussion of this case, see [15].

VII. Dispersion Effects

The presence of surface wave modes, especially the zero cutoff modes that exist in all finite substrate cases, contributes not only to power loss in the CPW mode but also to its dispersion.

When two modes with propagation constants k_1 and k_2 interact weakly in a transmission structure, their propagation constants are modified. Coupled mode theory predicts the modified propagation constants to be [17]

$$k' = \left[\frac{k_1 + k_2}{2} \pm \sqrt{\left(\frac{k_1 - k_2}{2} \right)^2 \pm C^2} \right] \tag{12}$$

where C is the mode coupling coefficient. This coefficient is a function of the field overlap integral I [18], given by

$$I = \int \left(\vec{E}_1 \times \vec{H}_2 \right) \cdot d\vec{s} \tag{13}$$

evaluated over the cross section of the waveguide. Subscripts 1 and 2 correspond to the two interacting modes.

Overlap integrals were calculated for the interactions of microstrip and CPW with surface wave and parallel-plate modes. The results were normalized with respect to the incident power, and give a comparison between the strengths of these interactions in various structures. The highest value of overlap was found to be between microstrip and the TE_0 mode. This value was selected as the normalizing reference for all the cases considered. Since the overlap integral is frequency dependent where non-TEM modes are involved, frequencies were selected close to the point where the propagation constant of the mode intersects that of CPW or microstrip.

The first structure considered is a 50 Ω microstrip line on a 100 μm substrate with a relative dielectric constant of 12.5. Field overlaps with TM_0 and TE_1 surface wave modes are given in Table I. The overlap with TM_0 is selected as unity for reference.

The next structure is a 50 Ω coplanar waveguide without back-side metallization. Two different values of $W+2G$ are considered. The results are given in Table II.

Finally, a 50 Ω coplanar waveguide with back-side metallization is considered. The overlap integrals for its interaction with parallel-plate modes are given in Table III.

It can be seen that coplanar waveguide field overlaps depend strongly on the value of $(W+2G)$. Practical coplanar waveguides with $(W+2G) \ll h$ interact less than microstrip lines with the first two TE and TM surface wave modes. In this respect the main difference between microstrip and coplanar waveguide is the degree of freedom in their physical layouts. On a given substrate material microstrip has two degrees of freedom: line width W and substrate thickness h. Changing both of these while keeping line impedance constant results only in a frequency

TABLE I
50 Ω MICROSTRIP ON 100 μm SUBSTRATE

Mode	Overlap
TM_0	1.00
TE_1	0.857

TABLE II
50 Ω COPLANAR WAVEGUIDE ON 400 μm SUBSTRATE

$W+2G(\mu m)$	Mode	Overlap
100	TM_0	0.353
100	TE_1	0.119
50	TM_0	0.213
50	TE_1	0.062

TABLE III
50 Ω GROUNDED COPLANAR WAVEGUIDE ON 400 μm SUBSTRATE

$W+2G(\mu m)$	Mode	Overlap
100	TEM	0.224
100	TM_1	0.559
100	TE_1	0.180
50	TEM	0.134
50	TM_1	0.371
50	TE_1	0.095

scaling and does not change the field overlaps. With coplanar waveguide, on the other hand, $(W+2G)$ can by varied independent of line impedance in order to minimize field overlap with surface wave modes and, therefore, to minimize dispersion. Some experimental results have been reported for the dispersion of coplanar waveguides [19]. As an extension of these results coplanar waveguides with $(W+2G)=h/8$ were fabricated on GaAs that showed no measurable dispersion in the frequency range of 10 to 100 GHz.

VIII. CONCLUSION

For coplanar waveguides, dispersion due to interaction with surface wave parallel-plate modes in the substrate strongly depends on the ground-to-ground spacing $(W+2G)$. If this spacing is small compared to dielectric wavelength and substrate thickness, both dispersion and radiation losses are minimized. In finite ground plane cases, the condition of small ground-to-ground spacing compared to substrate thickness is also necessary to avoid the excitation of the microstrip mode, and to minimize the deviation of the CPW mode from the "odd" mode of the ideal line.

Limitations on the reduction of $(W+2G)$ come from conductor loss, which imposes a minimum width requirement on the center conductor. If substrate thickness is to be kept large compared with this dimension, it is inevitable that at high frequencies the operation of CPW will not be below the cutoff frequency of surface wave modes. However, as was shown here, the interaction of the CPW mode with surface wave modes is negligible for integrated circuit applications if ground-to-ground spacing is small compared with dielectric wavelength.

ACKNOWLEDGMENT

The authors would like to express their thanks to Prof. B. A. Auld of Stanford University for valuable discussions.

REFERENCES

[1] M. Riaziat, I. Zubeck, S. Bandy, and G. Zdasiuk, "Coplanar waveguides used in 2–18 GHz distributed amplifier," in *1986 IEEE MTT-S Int. Microwave Symp. Dig.*, June 1986.

[2] M. Riaziat, S. Bandy, and G. Zdasiuk, "Coplanar waveguides for MMICs," *Microwave J.*, vol. 30, no. 6, June 1987.

[3] M. Riaziat, E. Par, G. Zdasiuk, S. Bandy, and M. Glenn, "Monolithic millimeter wave CPW circuits," in *1989 IEEE MTT-S Int. Microwave Symp. Dig.*, June, 1989, pp. 525–528.

[4] Y. C. Shih and T. Itoh, "Analysis of conductor backed coplanar waveguide," *Electron. Lett.*, vol. 18, no. 12, pp. 538–540, June 1982.

[5] R. W. Jackson, "Considerations in the use of coplanar waveguide for millimeter wave integrated circuits," *IEEE Trans. Microwave Theory Tech.*, vol. MTT-34, pp. 1450–1456, Dec. 1986.

[6] R. W. Jackson, "Mode conversion at discontinuities in finite width conductor backed coplanar waveguide," *IEEE Trans. Microwave Theory Tech.*, vol. 37, pp. 1582–1589, Oct. 1989.

[7] S. S. Bedair and I. Wolff, "Fast and accurate analytic formulas for calculating the parameters of a general broadside coupled coplanar waveguide for MMIC applications," *IEEE Trans. Microwave Theory Tech.*, vol. 37, pp 843–850, May 1989.

[8] G. Ghione and C. Naldi, "Analytical formulas for coplanar lines in hybrid and monolithic MICs," *Electron. Lett.*, vol. 20, no. 4, pp. 179–181, Feb. 1984.

[9] H. Shigesawa, M. Tsuji, and A. A. Oliner, "Conductor backed slotline and coplanar waveguide: Dangers and full wave analyses," in *1988 IEEE MTT-S Int. Microwave Symp. Dig.*, May 1988, pp. 199–202.

[10] Y. Fujiki, M. Suzuki, T. Kitazawa, and Y. Hayashi, "Higher order modes in coplanar type transmission lines," *Electron. and Commun. Japan*, vol. 58-B, no. 2, pp. 74–81, 1975.

[11] J. B. Knorr, and K. Kuchler, "Analysis of coupled slots and coplanar strips on dielectric substrate," *IEEE Trans. Microwave Theory Tech.*, vol. MTT-23, pp. 541–548, July 1975.

[12] C. P. Wen, "Coplanar waveguide: A surface strip transmission line suitable for nonreciprocal gyromagnetic device applications," *IEEE Trans. Microwave Theory Tech.*, vol. MTT-17, pp. 1087–1090, Dec. 1969.

[13] D. B. Rutledge, D. P. Neikirk, and D. P. Kasilingam, "Integrated circuit antennas," in *Infrared and Millimeter Waves*, vol. 10. New York: Academic Press, 1983.

[14] R. Collin, *Field Theory of Guided Waves*. New York: McGraw-Hill, 1960.

[15] M. Riaziat, I. J. Feng, R. Majidi-Ahy, and B. A. Auld, "Single mode operation of coplanar waveguides," *Electron. Lett.*, vol. 23, no. 24, Nov. 1987.

[16] K. D. Marx, "Propagation modes, equivalent circuits, and characteristic terminations for multiconductor transmission lines with inhomogeneous dielectrics," *IEEE Trans. Microwave Theory Tech.*, vol. MTT-21, pp. 450–457, July 1973.

[17] W. M. Louisell, *Coupled Mode and Parametric Electronics*. New York: Wiley, 1960.

[18] A. Hardy and W. Streifer, "Coupled mode theory of parallel waveguides," *J. Lightwave Technol.* vol. LT-3, pp. 1135–1146, Oct. 1985.

[19] R. Majidi-Ahy, K. Weingarten, M. Riaziat, D. Bloom, and B Auld, "Electrooptic sampling measurements of dispersion characteristics of slotline and coplanar waveguide even and odd modes," in *1988 IEEE MTT-S Int. Microwave Symp. Dig.*, May 1988, pp. 301–304.

Majid Riaziat (M'84) received the B.S. degree in engineering physics from the University of Oklahoma in 1978 and the M.S. and Ph.D. degrees in applied physics from Stanford University in 1980 and 1983 respectively.

In 1984 he joined the Varian Research Center in Palo Alto, CA, where he was responsible for the development of coplanar waveguide integrated circuits as well as InP-based HEMT's, MMIC's and OEIC's. His current research interests include millimeter-wave integrated circuits and high-speed optoelectronics.

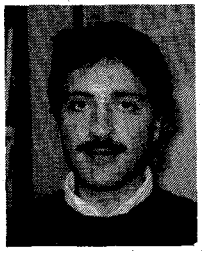

Reza Majidi-Ahy (M'82) was born in Tehran, Iran. He received the B.S.E.E. and M.S.E.E. degrees from the University of California at San Diego and the Ph.D. degree in electrical engineering from Stanford University. His thesis topic at Stanford was "100 GHz GaAs MMIC's, Electrooptic and Electronic Wafer Probes." He was also a recipient of a Rockwell International and Stanford Center for Integrated Systems fellowship.

He is currently with the Varian Research Center, Palo Alto, CA, where he conducts research on millimeter-wave electronic and high-speed optoelectronic InP and GaAs devices, MMIC's, and OEIC's. His research interests also include high-speed superconducting electronics and optoelectronics, and high-speed measurement techniques. Prior to his Ph.D. work at Stanford University, he was a senior research and development engineer at Microwave Technology Inc., Fremont, CA, and before that he was with Harris Microwave Semiconductor Inc., Milpitas, CA.

Dr. Majidi-Ahy has 14 publications and conference presentations, and a few patents.

I-Jaung Feng received the B.S. degree in physics from National Tsing-Hua University, Hsin Chu, Taiwan, in 1975, and the Ph.D. degree in physics and the M.S. degree in computer science from the University of Pittsburgh, Pittsburgh, PA, in 1982.

From 1982 to 1984, she was with AT&T Bell Labs at Murray Hill, NJ. Presently, she is a senior research engineer at the Varian Research Center, Palo Alto, CA. Her current research interests include electromagnetic theory, semiconductor device modeling, and numerical methods.